Modeling of Branching and Gelation in RAFT Copolymerization of Vinyl/Divinyl Systems

Rui Wang,[†] Yingwu Luo,*[,†] Bo-Geng Li,*[,†] and Shiping Zhu*[,‡]

Department of Chemical & Biochemical Engineering, State Key Laboratory of Chemical Engineering, Zhejiang University, Hangzhou, Zhejiang, P.R. China 310017, and Department of Chemical Engineering, McMaster University, Hamilton, Ontario, Canada L8S 4L7

Received September 2, 2008; Revised Manuscript Received November 7, 2008

ABSTRACT: The reversible addition−fragmentation chain transfer radical polymerization (RAFT) with branching/cross-linking is theoretically investigated on the basis of the method of moments. The system considered consists of the copolymerization of vinyl monomer in the presence of a small amount of divinyl comonomer. It is found that the gel point is significantly postponed by increasing the RAFT agent concentration. Flory's criterion, $\rho r_{w,0} = 1$, is found to be satisfied at the gel point in the RAFT cross-linking process regardless of the unequal reactivities of vinyl/divinyl monomers in the absence of cyclization. The gel conversion can be analytically expressed and is determined by the polymerization recipe and the relative reactivities of various double bonds. The gel point is postponed by the presence of intramolecular cyclization, and its effect becomes significant in a dilute polymerization system. Branching distribution is found to be very broad with a large fraction of linear primary and slightly branched chains. By the introduction of the dependence of the reactivity of the pendant double bond on the local heterogeneity, the branching distribution becomes narrower and can be fine-tuned.

Introduction

Copolymerization of vinyl monomer with a small amount of divinyl monomer causes cross-linking among different chains and produces branched polymers. Branched polymers that have high molecular weight and low viscosity are particularly useful as lubricants and coating materials because of their good mechanical properties and processing characteristics.[1] Successive intermolecular cross-linking rapidly increases the branched polymer molecular weight and yields gelation, that is, the formation of an insoluble 3D network. This critical transition from a highly branched polymer to a network is defined as the gel point.[2] Gel materials are widely used as ion-exchange resins, chromatography packings, and super absorbents.[3,4] In addition, they are used in many biomedical applications, such as contact lenses, drug delivery formulation, enzyme encapsulation, and tissue engineering.[5−7]

Depending on the targeted structure of final products (i.e., branched or gel polymer), the prediction of the gel point is critically important for determining polymerization recipes and operation conditions. Flory and Stockmayer made pioneering contributions to understanding the cross-linking process.[2,8,9] Their mean field theory assumes a random distribution of branching/cross-linking points and no intramolecular cyclization. It thus treats gelation as a process in thermodynamic equilibrium. According to Flory, the following simple relationship exists at the gel point

$$\rho r_{w,0} = 1 \tag{1}$$

where ρ is the branching/cross-linking density defined as the ratio of the number of branching points to that of the total monomeric units in macromolecules, and $r_{w,0}$ is the weight-average length of primary chains. (Note: In the vinyl/divinyl copolymerization, one cross-linkage, that is, a bridge between two primary chains, has two branching/cross-linking points; the terms branching point and cross-linking point are used interchangeably.) The physical meaning of eq 1 is that a gel molecule emerges when, by the weight average, each primary chain bears one branching/cross-linking point or half of a cross-linkage. Following the work of Flory and Stockmayer, many statistical models have been developed, such as those by Charlesby and Pinner,[10] Gordon,[11] Saito,[12] Macosko and Miller,[13,14] Pearson and Graessley,[15] Durand and Bruneau,[16] and so on. However, the branching/cross-linking process in free-radical polymerization (FRP) is inherently kinetically controlled. The development of polymer chain structural properties strongly depends on the reaction path. Peppas et al.[17] used a kinetic approach to take into account the reaction path effect. In addition, Tobita and Hamielec[18−20] made a rather comprehensive contribution to this end. The key part of the Tobita−Hamielec model is that it demonstrated the inherent inhomogeneity of polymer networks formed in the free-radical copolymerization process. Furthermore, Zhu et al.[21−23] employed the method of moments in investigating the validity of the monoradical assumption (i.e., no polymer chain bears more than one radical center) and the stationary-state hypothesis in modeling approaches. Although the reaction path has been included in the above kinetics models, there is no significant deviation from Flory's theory found in predicting the gel point when the intramolecular cyclization is not involved in the mechanism.

However, a number of experimental studies showed that the network formed in a conventional free-radical process is largely deviated from Flory's mean field theory.[24−28] For example, the occurrence of gelation that was observed in the experiment was significantly postponed, and the critical numbers of branching/cross-linking points at the gel point were typically one or two orders of magnitude larger than those predicted by Flory's theory. This discrepancy is mainly attributed to intramolecular cyclization neglected in the classical theory. Intramolecular cyclization was observed at the beginning of polymerization, which is related to chemical and physical characteristics of the conventional free-radical process. Slow initiation and fast chain propagation in the free-radical polymerization result in the formation of polymer chains having high molecular weight and bearing numerous pendant double bonds at low conversions.

* Corresponding authors. (Y.L.) E-mail: yingwu.luo@zju.edu.cn, Tel: 86-571-87951832, Fax: 86-571-87951612. (B.L.) E-mail: bgli@zju.edu.cn, Tel: 86-571-87952623, Fax: 86-571-87951612. (S.Z.) E-mail: zhuship@macmaster.ca, Tel: (905) 525-9140 ext. 24962, Fax: (905) 521-1350.

[†] Zhejiang University.

[‡] McMaster University.

10.1021/ma802006c CCC: $40.75
Published on Web 12/03/2008

These long chains do not overlap each other in a dilute solution because of the excluded volume effect. In addition, slow rates of diffusion and relaxation of long polymer chains relative to the fast propagation reduce the probability of sufficient contacts between functional groups on different chains. These characteristics promote intramolecular cyclization because the radical center is surrounded by pendant double bonds belonging to the same chain. Therefore, highly cross-linked domains (i.e., microgels) are formed at the low concentration of polymer chains, which are further linked with each other through intermolecular reactions and finally form networks on a macroscopic scale. The network formed by the conventional free-radical cross-linking process is therefore highly inhomogeneous.[29,30]

The recently developed control/living radical polymerization (CLRP) techniques, including nitroxide-mediated polymerization (NMP), atom transfer radical polymerization (ATRP), and reversible addition fragmentation chain transfer polymerization (RAFT), have been widely used in controlling the molecular weight distribution and architecture of polymer chains.[31−34] In CLRP, the growth of individual polymer chains is slow (in hours in contrast to seconds in the conventional FRP) and can be divided into numerous sections because of a rapid reversible activation/deactivation process, which guarantees an equal probability for each chain to grow.[35] The CLRP is also expected to be advantageous in the cross-linking process. In CLRP, there is a huge number of chains of low molecular weight in the system. These short chains tend to penetrate each other. In addition. the slow growth gives chains sufficient time for relaxation and diffusion, which facilitates the functional groups (i.e., radical centers and pendant double bonds) in the polymerization system to contact each other. This favors intermolecular cross-linking and suppresses the formation of microgels. Therefore, the CLRP cross-linking process provides a good model for testing Flory's mean field theory because the assumptions are likely to be more satisfied. Recently, several research groups have successfully synthesized branched polymers or gels by NMP, ATRP, and RAFT techniques.[36−51] Fukuda and coworkers[37] found that the critical cross-link density at the gel point agrees with Flory's theory by a factor of two in an NMP cross-linking system. Matyjaszewski et al.[44] observed similar results in an ATRP system. Zhu et al.[40] reported that the copolymerization of MMA and EGDMA has the gel conversions very close to the values predicted by the Flory's theory. Armes et al.[49] found that the gel point depends on the structure of cross-linkers (the type of divinyl monomer). In addition, by measuring the swelling ratio and the loss tangent peak, respectively, Fukuda et al.[37] and Zhu et al.[42] demonstrated that the gels prepared by CLRP methods are more homogeneous in terms of network microstructure than those by conventional FRP processes.

Although significant progress has been achieved in understanding and applying CLRP cross-linking processes through experimental approaches, there is still a lack of theoretical study on the kinetics of these processes and the structure of the network products. In this article, we develop a kinetic model for describing the RAFT cross-linking process using the method of moments. The effect of RAFT process on gelation is investigated using the model. In addition, we provide an analytical expression of the gel point, which is determined by the initial copolymerization recipe. Moreover, the intramolecular cyclization is taken into account in the cross-linking mechanism, and its effect on the gelation process is studied. Finally, we investigate the branching development and distribution in the RAFT cross-linking process.

Table 1. Elementary Reactions of Vinyl/Divinyl RAFT Copolymerization

initiation	$I \xrightarrow{f,k_d} 2P_{0,1,0}$	(I)
	$P_{0,1,0} + M_i \xrightarrow{k_{p,i}} P_{1,1,0}$	(II)
propagation with comonomer	$P_{n,r,c} + M_i \xrightarrow{k_{p,i}} P_{n+1,r,c}$	(III)
transfer to RAFT species	$P_{n,r,c} + P_{m,s,d} \xrightarrow{rdk_{tr}} P_{n,r-1,c+1} + P_{m,s+1,d-1}$	(IV)
termination by disproportionation	$P_{n,r,c} + P_{m,s,d} \xrightarrow{rsk_{td}} P_{n,r-1,c} + P_{m,s-1,d}$	(V)
termination by recombination	$P_{n,r,c} + P_{m,s,d} \xrightarrow{rsk_{tc}} P_{n+m,r+s-2,c+d}$	(VI)
propagation with pendant double bond	$P_{n,r,c} + P_{m,s,d} \xrightarrow{rmk_{inter}} P_{n+m,r+s,c+d}$	(VII)

Model Development for RAFT Branching/Cross-Linking Process. This model is an extension of Zhu's previous kinetic work on the conventional vinyl/divinyl copolymerization.[21] In applying it to the RAFT process, we must distinguish the end unit of a primary chain between the radical center and the RAFT species. Here we use $P_{n,r,c}$ to denote the macromolecule containing n monomeric units, r radical centers, and c RAFT moieties. The elementary reactions of the RAFT cross-linking process are listed in Table 1, where I and M_i represent thermal initiator and monomer i, respectively (M_1 is vinyl monomer, and M_2 is divinyl monomer).

It should be pointed out that for simplicity we employed two approximations in the above mechanism. First, we neglected the intermediate radicals and their cross-termination reactions[52−54] because they greatly increase the dimension of variables and are difficult in mathematical manipulation. This simplification is acceptable in the cross-linking process as far as the gel conversion is concerned. We will clarify this point in the following section. Second, we used the pseudokinetic rate constant method that was suggested by Tobita and Hamielec to treat the copolymerization.[18] Strictly speaking, this assumption is valid only when chains are long or when copolymer composition is far from 0.5. In the RAFT cross-linking process, the amount of divinyl monomer is small, and thus errors are minor. Under this approximation, the rate constants in Table 1 are the functions of radical fractions, ϕ_i, which can be calculated by the instantaneous monomer composition, f_i, through a long-chain assumption. The pseudo rate constants of propagation with M_i ($k_{p,i}$), transfer to RAFT (k_{tr}), termination (k_t), and propagation with pendant double bond (k_{inter}) are expressed as

$$k_{p,i} = \sum_j k_{p,ij}\varphi_j \tag{1a}$$

$$k_{tr} = \sum_j k_{tr,j}\varphi_j \tag{1b}$$

$$k_t = \sum_i \sum_j k_{t,ij}\varphi_i\varphi_j \tag{1c}$$

$$k_{inter} = \sum_j k^*_{p,j}\varphi_j(\bar{F}_2 - \bar{C}) \tag{1d}$$

where $\bar{F}_2$ is the divinyl density in the total copolymer and $\bar{C}$ is the cross-linkage density, which equals half of the branching

density ρ in Flory's theory. On the basis of this mechanism, the population balance for $P_{n,r,c}$ is

$$\frac{dP_{n,r,c}}{dt} = \sum_i k_{p,i}M_iP_{n-1,r,c} - \sum_i k_{p,i}M_iP_{n,r,c} + \sum_{m=0}^{\infty}\sum_{s=0}^{\infty}\sum_{d=1}^{\infty}(r+1)dk_{tr}P_{n,r+1,c-1}P_{m,s,d} - \sum_{m=0}^{\infty}\sum_{s=0}^{\infty}\sum_{d=1}^{\infty}rdk_{tr}P_{n,r,c}P_{m,s,d} + \sum_{m=0}^{\infty}\sum_{s=1}^{\infty}\sum_{d=0}^{\infty}s(c+1)k_{tr}P_{n,r-1,c+1}P_{m,s,d} - \sum_{m=0}^{\infty}\sum_{s=1}^{\infty}\sum_{d=0}^{\infty}sck_{tr}P_{n,r,c}P_{m,s,d} + \sum_{m=0}^{\infty}\sum_{s=1}^{\infty}\sum_{d=0}^{\infty}(r+1)sk_{td}P_{n,r+1,c}P_{m,s,d} - \sum_{m=0}^{\infty}\sum_{s=1}^{\infty}\sum_{d=0}^{\infty}rsk_{td}P_{n,r,c}P_{m,s,d} + \frac{1}{2}\sum_{m=0}^{n}\sum_{s=1}^{r+1}\sum_{d=0}^{\infty}(r+2-s)sk_{tc}P_{m,s,d}P_{n-m,r+2,c-d} - \sum_{m=0}^{\infty}\sum_{s=1}^{\infty}\sum_{d=0}^{\infty}rsk_{tc}P_{n,r,c}P_{m,s,d} + \sum_{m=0}^{n}\sum_{s=0}^{r}\sum_{d=0}^{c}s(n-m)k_{p,inter}P_{m,s,d}P_{n-m,r-s,c-d} - \sum_{m=0}^{\infty}\sum_{s=0}^{\infty}\sum_{d=0}^{\infty}rmk_{p,inter}P_{n,r,c}P_{m,s,d} - \sum_{m=0}^{\infty}\sum_{s=1}^{\infty}\sum_{d=0}^{\infty}snk_{p,inter}P_{n,r,c}P_{m,s,d} \quad (2)$$

We resort to the method of moments to avoid solving this set of an indefinite number of ODEs. Let us define the moments of $P_{n,r,c}$ as

$$Y_{i,j,k} = \sum_{n=0}^{\infty}\sum_{r=0}^{\infty}\sum_{c=0}^{\infty}n^ir^jc^kP_{n,r,c} \quad (3)$$

All sums in eq 3 are from 0 because we assume chain-structure-independent kinetic parameters. After lengthy but straightforward algebra, eq 2 can be transformed to the moment equations listed in Table 2. By solving these equations, we can track the time evolution of each chain moment. More importantly, some characteristics reflecting the process of cross-linking and the evolution of the chain/network structure can be obtained by the combination of these moments, as listed in Table 3. The gel point is defined as the moment at which the weight-average chain length, r_w, approaches infinite.

The rate constant values used in this simulation are listed in Table 4. They are approximated to those of the real polymerization systems in order of magnitude.[35,55,56] Here for simplicity, we assume that their values are independent of the type of radicals. In addition, we also assume equal reactivity of the double bonds (i.e., $k_{p,1} = 0.5k_{p,2} = k_p^*$). It should be pointed out that the equal reactivity assumption does not mean that there is random distribution of pendant double bonds along primary chains because the priority of divinyl to be consumed causes composition drifting.

The weight-average primary chain length ($r_{w,0}$) is required for the comparison of our simulation results with the Flory–Stockmayer theory. This quantity can be obtained through the above model by simply setting $k_{p,j}^* = 0$. Finally, it should be noted that we do not take the intramolecular cyclization into consideration in the basic model presented here. However, this side reaction can be easily included in this model, as discussed in the following part.

Table 2. Moment Equations in the RAFT Cross-Linking Process

zeroth-order moments	$dY_{0,0,0}/dt = 2fk_d[I] - {}^1/_2k_{tc}Y_{0,1,0}^2 - k_{p,inter}Y_{1,0,0}Y_{0,1,0}$
first-order moments	$dY_{1,0,0}/dt = \sum_i k_{p,i}M_iY_{1,0,0}$
	$dY_{0,1,0}/dt = 2fk_d[I] - k_{td}Y_{0,1,0}^2 - k_{tc}Y_{0,1,0}^2$
	$dY_{0,0,1}/dt = 0$
second-order moments	$dY_{2,0,0}/dt = 2\sum_i k_{p,i}M_iY_{1,1,0} + \sum_i k_{p,i}M_iY_{0,1,0} + k_{tc}Y_{1,1,0}^2 + 2k_{p,inter}Y_{1,1,0}Y_{2,0,0}$
	$dY_{0,2,0}/dt = 2fk_d[I] - 2k_{td}Y_{0,2,0}Y_{0,1,0} + k_{td}Y_{0,1,0}^2 + 2k_{tc}Y_{0,1,0}^2 - 4k_{tc}Y_{0,2,0}Y_{0,1,0} + k_{tc}Y_{0,2,0}^2 - 2k_{tr}Y_{0,2,0}Y_{0,0,1} + 2k_{tr}Y_{0,1,0}Y_{0,0,1} + 2k_{tr}Y_{0,1,1}Y_{0,1,0} + 2k_{p,inter}Y_{0,2,0}Y_{1,1,0}$
	$dY_{0,0,2}/dt = k_{tc}Y_{0,1,1}^2 - 2k_{tr}Y_{0,0,2}Y_{0,1,0} + 2k_{tr}Y_{0,1,1}Y_{0,0,1} + 2k_{tr}Y_{0,1,0}Y_{0,0,1} + 2k_{p,inter}Y_{0,1,1}Y_{1,0,1}$
	$dY_{1,1,0}/dt = \sum_i k_{p,i}M_iY_{0,2,0} - k_{td}Y_{1,1,0}Y_{0,1,0} + k_{tc}Y_{1,1,0}Y_{0,2,0} - 2k_{tc}Y_{1,1,0}Y_{0,1,0} - k_{tr}Y_{1,1,0}Y_{0,0,1} + k_{tr}Y_{1,0,1}Y_{0,1,0} + k_p^*Y_{2,0,0}Y_{0,2,0} + k_{p,inter}Y_{1,1,0}^2$
	$dY_{1,0,1}/dt = \sum_i k_{p,i}M_iY_{0,1,1} + k_{tc}Y_{1,1,0}Y_{0,1,1} + k_{tr}Y_{1,1,0}Y_{0,0,1} + k_{tr}Y_{1,0,1}Y_{0,1,0} + k_{p,inter}Y_{2,0,0}Y_{0,1,1} + k_{p,inter}Y_{1,1,0}Y_{1,0,1}$
	$dY_{0,1,1}/dt = -k_{td}Y_{0,1,1}Y_{0,1,0} + k_{tc}Y_{0,1,1}Y_{0,2,0} - 2k_{tc}Y_{0,1,1}Y_{0,1,0} + k_{tr}Y_{0,2,0}Y_{0,0,1} + k_{tr}Y_{0,0,2}Y_{0,1,0} - k_{tr}Y_{0,1,1}Y_{0,0,1} - k_{tr}Y_{0,1,1}Y_{0,1,0} - 2k_{tr}Y_{0,1,0}Y_{0,0,1} + k_{p,inter}Y_{0,1,1}Y_{1,1,0} + k_{p,inter}Y_{0,2,0}Y_{1,0,1}$
small molecules	initiator: $d[I]/dt = -k_d[I]$
	monomer: $d[M_i]/dt = -k_{p,i}Y_{0,1,0}[M_i]$
intermolecular cross-linkage	$d[C]/dt = k_{p,inter}Y_{1,0,0}Y_{0,1,0}$

Table 3. Definition of Important Chain Structural Properties

chain property	expression
number-average chain length	$r_n = Y_{1,0,0}/Y_{0,0,0}$
weight-average chain length	$r_w = Y_{2,0,0}/Y_{1,0,0}$
polydispersity index	$PDI = \bar{r}_W/\bar{r}_N$
radical distribution index	$RDI = Y_{0,2,0}/Y_{0,1,0}$
number-average branching density	$B_n = Y_{0,0,1}/Y_{0,0,0} - 1$
weight-average branching density	$B_w = Y_{1,0,1}/Y_{1,0,0} - 1$
density of intermolecular cross-links	$\bar{C} = [C]/Y_{1,0,0}$

Table 4. Rate Constants Used in the Simulation

kinetics constants	values[a]
initiator decomposition: k_d	10^{-5} s^{-1}
initiator efficiency: f	0.5
propagating with monovinyl: $k_{p,1j}$	1×10^3 L·mol^{-1}·s^{-1}
propagating with divinyl: $k_{p,2j}$	2×10^3 L·mol^{-1}·s^{-1}
propagating with pendant double bond: $k_{p,j}^*$	1×10^3 L·mol^{-1}·s^{-1}
transfer to RAFT agent: $k_{tr,j}$[b]	1×10^6 L·mol^{-1}·s^{-1}
termination: k_{tc}, k_{td}	1×10^7 L·mol^{-1}·s^{-1}

[a] An approximate system is MMA/EGDMA copolymerization with 2-cyranoprop-2-yl dithiobenzoate (CPDB) as RAFT agent. [b] The $k_{tr,j}$ value is adjusted when the effect of chain transfer coefficient on gelation is investigated. Otherwise, it remains 1×10^6 L·mol^{-1}·s^{-1}.

Results and Discussion

Effect of RAFT Process on Cross-Linking Kinetics. At first, we investigate the effect of RAFT agent concentration on the cross-linking process. In the simulation, we set the initial vinyl concentration $[M_1]_0$ to 6 mol/L and keep the initial mole ratios of $M_2/M_1$and I/M_1 to 2 and 0.2%, respectively. It is evident in Figure 1a that the occurrence of gel point is dramatically postponed when the RAFT agent is added to the copolymerization system. For the cross-linking without RAFT agent, gelation occurs at the very beginning of polymerization (i.e., <0.1% in monomer conversion). In contrast, when $[RAFT]_0/[M_2]_0$ increases from 0.2 to 1 to 2, the gel conversion is

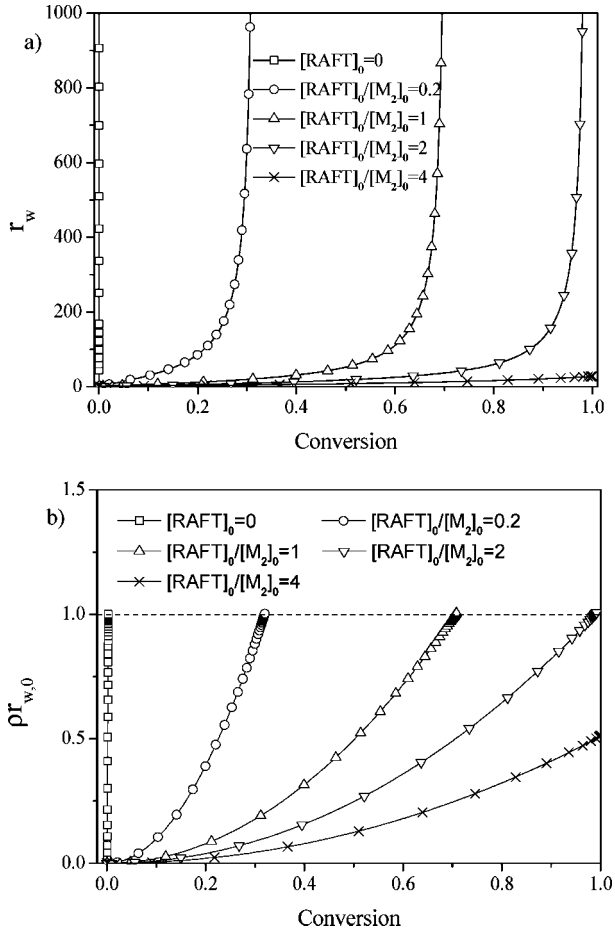

Figure 1. Effect of RAFT agent concentration on cross-linking process: (a) r_w versus monomer conversion and (b) $\rho r_{w,0}$ versus monomer conversion. (Flory's criterion is noted as the dashed line.) $[M_1]_0 = 6$ mol/L, $[M_2]_0 = 2\%[M_1]_0$, and $[I]_0 = 0.2\%[M_1]_0$.

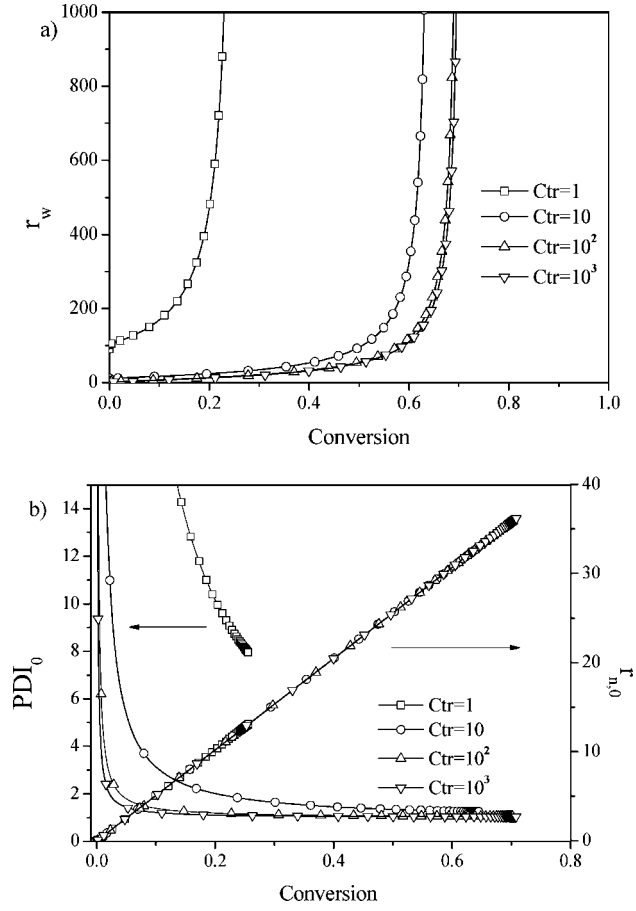

Figure 2. Effect of RAFT chain transfer coefficient on cross-linking process: (a) r_w versus monomer conversion and (b) number-average chain length and polydispersity of primary chain versus monomer conversion. $[M_1]_0 = 6$ mol/L, $[M_2]_0 = 2\%[M_1]_0$, $[\text{RAFT}]_0 = 2\%[M_1]_0$, and $[I]_0 = 0.2\%[M_1]_0$.

postponed to 0.32, 0.71, and 0.99, respectively. For the system of $[\text{RAFT}]_0/[M_2]_0 = 4$, gelation does not occur, even when all of the monomers are consumed, and the average chain length increases almost linearly with the monomer conversion.

Flory[2] suggested that $\rho r_{w,0} = 1$ could be used as a criterion for the gel point. It can be seen in Figure 1b that Flory's criterion is valid for predicting the gel point in the RAFT cross-linking process if the intramolecular cyclization is absent. $\rho r_{w,0}$ steadily increases with monomer conversion and approaches unity at the gel point. However, if $\rho r_{w,0} < 1$ in the final stage of polymerization (as in the case of $[\text{RAFT}]_0/[M_2]_0 = 4$), then no gelation occurs. The postponed gel point caused by the RAFT agent can be explained according to Flory's criterion. The high RAFT agent concentration yields more primary chains and thus decreases their chain lengths, $r_{w,0}$, at the same monomer conversion. Moreover, the branching density, ρ, is determined by only the copolymerization and cross-linking kinetics and not by the RAFT process. (See the Analytical Description.) As a result, the value of $\rho r_{w,0}$ decreases as $[\text{RAFT}]_0$ increases. The postponed gel point in RAFT follows the same principle as the addition of a large amount of initiator or chain-transfer agent in conventional radical polymerization. However, the resulting network is more homogeneous because primary chains are formed gradually instead of instantaneously.

The chain transfer coefficient, C_{tr} ($= k_{tr}/k_p$), is an important parameter in the RAFT process, which determines the chain length distribution in linear chain systems.[57] Here we investigate the effect of C_{tr} on the cross-linking process (as shown in Figure 2). Figure 2a shows that the gel conversion increases as C_{tr} decreases, especially when C_{tr} is small. However, when its value becomes adequately large (i.e., $C_{tr} > 10$), its effect on the gel point becomes minor. Figure 2b shows the effect of C_{tr} on the primary chain length. With all of the C_{tr} values, the number-average chain length $r_{n,0}$ increases linearly with the monomer conversion following the same theoretical line. However, C_{tr} has a significant effect on the polydispersity of primary chains PDI_0, as shown in Figure 2b. PDI_0 decreases as C_{tr} increases, and the effect becomes minor when $C_{tr} > 10$. This result is in agreement with the previous work of Fukuda et al.[35] and Monteiro et al.[58] The increase in C_{tr} leads to the decrease in $r_{w,0}$ because $r_{w,0} = (r_{n,0})(\text{PDI}_0)$. The gel point is thus postponed by increasing C_{tr} according to Flory's criterion. Because different C_{tr} values correspond to different types of RAFT agent, the simulation results indicate that the gel point also depends on the choice of RAFT agent type.

In Figure 3, we investigate the effect of initiator concentration on the gel point by adjusting $[I]_0$ by three orders of magnitude. This adjustment of $[I]_0$ in the simulation recipe brings about a 30-fold variation in the radical concentration, $[R]$, because $[R]$ is proportional to $[I]_0^{0.5}$. However, it is clearly seen in Figure 3 that there is no effect on gel conversion. This result will be further confirmed in the Analytical Description. The insensitivity of the gel point on $[R]$ indirectly proves that it is reliable to neglect intermediate radicals and their cross termination in modeling the RAFT cross-linking process. The presence of intermediate radicals can possibly facilitate cross termination with propagating radicals, which significantly reduces $[R]$.[54] However, the intermediate radicals cannot propagate with the

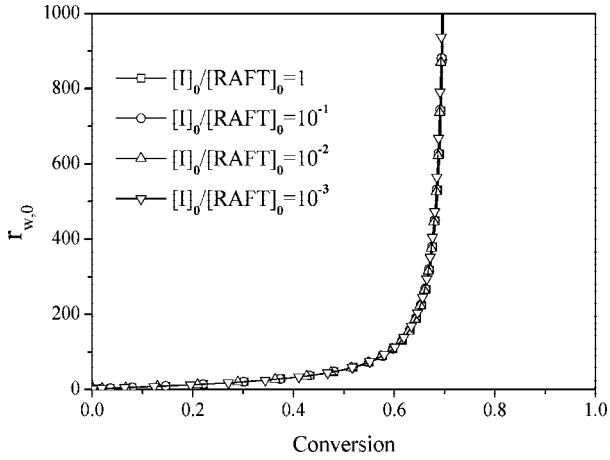

Figure 3. Effect of initiator concentration on cross-linking process. $[M_1]_0 = 6$ mol/L, $[M_2]_0 = 2\%[M_1]_0$, and $[\text{RAFT}]_0 = 2\%[M_1]_0$.

monomer as well as the pendant double bond and do not produce additional cross-links. Although cross termination yields additional branch points, its rate is much lower than propagation with pendant double bonds and is at the same level as combination termination (i.e., $k_{ct}[R][Y] \approx k_{tc}[R]^2 \ll k_p^*[R][M_2] \approx k_p^*[R][M_P]$, where $[Y]$and $[M_P]$ are the intermediate radical and pendant double bond concentrations). The number of cross-links produced by intermediate/propagating radical cross-termination is thus negligible. The sole effect of cross termination on $[R]$ does not change the gel point, as illustrated in Figure 3. The present model is reliable as far as the gel conversion is concerned. However, it could be erroneous in predicting gel time, particularly, in the presence of rate retardation.

Analytical Description. The consumption rate of vinyl and divinyl monomers can be denoted as

$$\frac{d[M_1]}{dt} = -k_{p,1}[R][M_1] \text{ or } \frac{dx_1}{dt} = k_{p,1}[R](1-x_1) \quad (4a)$$

$$\frac{d[M_2]}{dt} = -k_{p,2}[R][M_2] \text{ or } \frac{dx_2}{dt} = k_{p,2}[R](1-x_2) \quad (4b)$$

where x_1 and x_2 are the vinyl and divinyl monomer conversions, respectively. By dividing eq 4b by eq 4a and then integrating, we have

$$x_2 = 1 - (1-x_1)^{1/\alpha} \quad (5)$$

where α is a group parameter defined as $k_{p,2}/k_{p,1}$. From eq 5, we can see that $x_2 > x_1$ when $\alpha > 1$. This indicates that the divinyl monomer consumes faster than the vinyl monomer does, which causes a composition drifting along the primary chains. In the absence of intramolecular cyclization, the formation of the cross-link can be written as

$$\frac{d[C]}{dt} = k_p^*[R]([M_2]_0 x_2 - [C]) \quad (6)$$

By inserting eqs 4a and 5 into eq 6 and integrating, we obtain

$$\frac{[C]}{[M_2]_0} = \frac{\alpha\beta}{\alpha-\beta}\left[\frac{(1-x_1)^\alpha}{\alpha} - \frac{(1-x_1)^\beta}{\beta} + \frac{\alpha-\beta}{\alpha\beta}\right] \quad (7)$$

where β is another group parameter defined as $k_p^*/k_{p,1}$. It can be clearly seen from eq 7 that the cross-link concentration is determined by only the initial divinyl concentration, the monomer conversion, and two group parameters, but it is independent from the radical concentration. In addition, the RAFT process has no effect on the formation of cross-links.

In the RAFT cross-linking process, Flory's criterion can be transformed as

$$\rho\bar{r}_{w,0} = 2\bar{C}\bar{r}_{w,0} = \left(\frac{2[C]}{Y_{1,0,0}/\bar{r}_{n,0}}\right)\left(\frac{\bar{r}_{w,0}}{\bar{r}_{n,0}}\right) \approx \frac{2[C]\text{PDI}_0}{[\text{RAFT}]_0} = 1 \quad (8)$$

where $Y_{1,0,0}/\bar{r}_{n,0}$ represents the primary chain concentration, and it can be approximated to $[\text{RAFT}]_0$ because the fraction of primary chains originated from the initiator is negligible compared with that from the RAFT agent. In addition, we assume that $\text{PDI}_0 = 1$ because of the narrow length distribution of primary chains in the RAFT process (a large C_{tr} is assumed) and further simplify eq 8 as

$$\frac{[C]}{[\text{RAFT}]_0} = \frac{1}{2} \quad (9)$$

Equation 9 is equivalent to Flory's criterion in the RAFT cross-linking process, which indicates that the gel molecules emerge when the number of cross-link points accumulates to half of the RAFT agent concentration. By inserting the eq 7 into eq 9, we get an implicit expression of gel conversion

$$\frac{[M_2]_0}{[\text{RAFT}]_0} = \frac{1}{2}\frac{\alpha-\beta}{\alpha\beta}\left[\frac{(1-x_{1,\text{gel}})^\alpha}{\alpha} - \frac{(1-x_{1,\text{gel}})^\beta}{\beta} + \frac{\alpha-\beta}{\alpha\beta}\right]^{-1} \quad (10)$$

where $x_{1,\text{gel}}$ is the vinyl monomer conversion at the gel point. We compare this analytical result with the numerical solution by adjusting the α and β values, respectively, as shown in Figure 4. It can be seen that for all of the combinations of α and β, the simple analytical solutions obtained from eq 10 are in good agreement with the results from numerically solving the full set of moment equations. Therefore, for the RAFT cross-linking process without intramolecular cyclization, the gel point can be readily predicted by eq 10 if we know the polymerization recipe ($[M_2]_0/[\text{RAFT}]_0$) and the relative reactivities of vinyl, divinyl, and pendant double bond (α, β).

Figure 4 also shows that for all of the α and β values, the gel conversion monotonously decreases with the increase in $[M_2]_0/[\text{RAFT}]_0$, and all of the theoretical lines start at the point of $x_{1,\text{gel}} = 1$, $[M_2]_0/[\text{RAFT}]_0 = 0.5$. This result indicates that in the absence of intramolecular cyclization gelation occurs only if $[M_2]_0/[\text{RAFT}]_0 \geq 0.5$. In addition, it can be seen in Figure 4a that gelation occurs at lower conversions with larger α values. The large α value represents fast consumption of divinyl monomer, which increases the cross-linking density and thus makes $x_{1,\text{gel}}$ decrease. Moreover, Figure 4b shows that gelation also occurs earlier with larger β. The increase in β accelerates the conversion of the pendant double bond to become a cross-linkage, which results in an earlier gelation.

With the assumption of equal reactivity (i.e., $\alpha = 2$, $\beta = 1$), eq 10 can be further simplified to

$$x_{1,\text{gel}} = (2[M_2]_0/[\text{RAFT}]_0)^{-1/2} \quad (11)$$

An examination of the equation derivation reveals that the application of eqs 10 and 11 is not restricted to the RAFT cross-linking process but can be readily extended to other controlled/living radical cross-linking processes. We can simply replace $[\text{RAFT}]_0$ in the equations by the initiator concentration in the ATRP and NMP processes. Using these analytical equations, we can readily estimate the gel point from the polymerization recipe. In addition, it also allows us to optimize the cross-linking recipe for a targeted structure (i.e., gel or highly branched polymers). Finally, it should be pointed out that the presence of intramolecular cyclization affects the validity of eqs 10 and 11. We discuss the influence of this side reaction in the next section.

Effect of Intramolecular Cyclization on Gel Point. In the conventional radical cross-linking process, it is difficult for different chains to penetrate each other, and thus a radical center is surrounded by pendant double bonds belonging to the same chain. As a result, significant intramolecular cyclization occurs, which causes the deviation of gel conversion from the Flory's theory. In the cross-linking CLRP, the intramolecular reaction is reduced because of sufficient chain diffusion and relaxation and thus the uniform distribution of reactive species. However, several groups observed that the number of cross-links per primary chain in NMP, ATRP, and RAFT cross-linking processes is still slightly higher than Flory's prediction (i.e., 0.5, as in eq 9).[37,44] Some intramolecular cyclization is present in the CLRP systems. The effect of this side reaction on the RAFT cross-linking is theoretically investigated in this work. For simplicity, we neglect the configuration dependence of the intramolecular cyclization and describe the reaction as a monomolecular reaction.

$$P_{n,r,c} \xrightarrow{rnk_{intra}} P_{n,r,c} \qquad \text{(VIII)}$$

Because the numbers of monomeric units, radicals, and RAFT moieties are not changed after the intramolecular cyclization, this additional reaction has no influence on the moment equations listed in Table 2. However, this side reaction produces additional intramolecular cross-links and consumes pendant double bonds. On the basis of reaction VIII, the number of intramolecular cross-links, D, accumulates as

$$\frac{d[D]}{dt} = k_{intra} Y_{1,1,0} \qquad (12)$$

k_{intra} is the pseudo rate constant of intramolecular cyclization, which can be expressed as

$$k_{intra} = \sum_j k^*_{intra,j} \varphi_j (\bar{F}_2 - \bar{C} - \bar{D}) \qquad (13a)$$

where $k^*_{intra,j}$ is the rate coefficient of radical propagation with intramolecular pendant double bond, and $\bar{D}$ is the intramolecular cross-link density (i.e., $\bar{D} = [D]/Y_{1,0,0}$). The pseudo rate constant of intermolecular cross-linking, k_{inter}, should also be modified as

$$k_{inter} = \sum_j k^*_{p,j} \varphi_j (\bar{F}_2 - \bar{C} - \bar{D}) \qquad (13b)$$

Here we assume that $k^*_{intra,j}$ is independent from the type of radical center and investigate its effect on the gel point (as shown in Figure 5a). We also calculate the evolution of intermolecular and intramolecular cross-links per primary chain in Figure 5b to assist in understanding the mechanism. The simulation results show that when $k^*_{intra,j} = 0$, the gel conversion is ~50%, and the number of intermolecular cross-links per primary chain equals 0.5 at the gel point, which accords with Flory's theory. The gel conversion is postponed by only 2% when $k^*_{intra,j} = 10$ s^{-1}. In addition, the fraction of intramolecular cross-links is very small, which does not affect the increase in intermolecular cross-links. Moreover, when $k^*_{intra,j}$ increases to 50 s^{-1}, it is clearly seen in Figure 5a that the evolution of r_w exhibits an inflection after it rapidly increases to the 10^4 order of magnitude. These highly branched macromolecules contain multiple radical centers and pendant double bonds, which increase the probability of undergoing intramolecular cyclization. Figure 5b shows that the accumulation rate of intramolecular cross-links is much higher than that of intermolecular cross-links after the inflection. The increase in r_w slows down, and thus the gel point is postponed to 70% monomer conversion. Furthermore, this postponed gelation becomes more obvious when $k^*_{intra,j}$ increases to 100 s^{-1}. The gel conversion increases to almost 100%, and the final

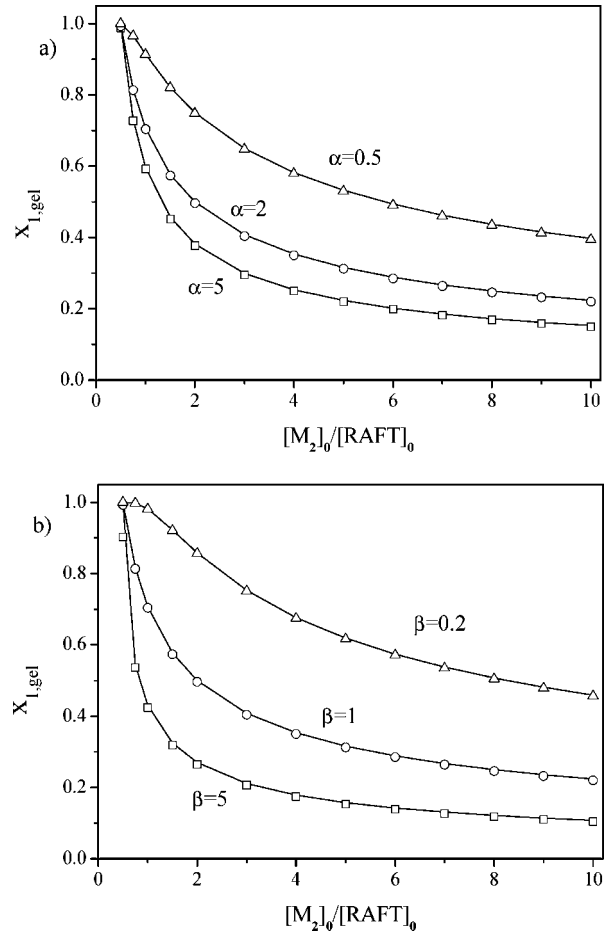

Figure 4. Comparison between analytical results and numerical solutions. $[M_1]_0 = 6$ mol/L, $[RAFT]_0 = 2\%[M_1]_0$, and $[I]_0 = 0.2\%[M_1]_0$. (a) Set $\beta = 1$ and adjust α. (b) Set $\alpha = 2$ and adjust β. The solid lines are the analytical results of eq 10, and the symbols are the numerical solutions of the moment equations.

number of intramolecular cross-links is almost three times as many as that of intermolecular cross-links. Finally, when $k^*_{intra,j}$ increases to 200 s^{-1}, the intramolecular cross-links accumulate very fast; as a result, there are not enough pendant double bonds for intermolecular cross-linking. No gelation occurs after all of the monomers are consumed. The cross-linking process stays in the stage of forming highly branched macromolecules.

Figure 6 is the gel diagram showing the dependence of $x_{1,gel}$ on $[M_2]_0/[RAFT]_0$ in the presence of intramolecular cyclization. It is clearly seen that the gel points are postponed by the intramolecular reaction for all of the values of $[M_2]_0/[RAFT]_0$. In addition, the gel conversion is more sensitive to the increase in k^*_{intra} when $[M_2]_0/[RAFT]_0$ is small because the number of pendant double bonds is limited in this case. Moreover, this gel diagram shows that the critical value of $[M_2]_0/[RAFT]_0$ that is required to cause gelation (i.e., its corresponding value at $x_{1,gel} = 1$) increases with $k^*_{intra,j}$. When $k^*_{intra,j} = 0$, $[M_2]_0/[RAFT]_0 \geq 0.5$ is sufficient for guaranteeing the occurrence of gelation. However, when $k^*_{intra,j}$ increases to 30, 50, 100, and 200 s^{-1}, the values of $[M_2]_0/[RAFT]_0$ should be at least 1, 1.35, 2, and 3.5, respectively, to reach the gel point. This simulation result is in good agreement with the recent experiment work of Armes et al.[49] They used the RAFT technique to copolymerize 2-hydroxyisopropyl acrylate (HPA) and three kinds of diacrylate cross-linkers (BEDA, DSDA, and EGDA). They found that gelation occurs when $[BEDA]_0/[RAFT]_0 \geq 1.35$, $[DSDA]_0/[RAFT]_0 \geq 1.5$, and $[EGDA]_0/[RAFT]_0 \geq 2.25$, respectively. This experimental result shows that the system with BEDA may

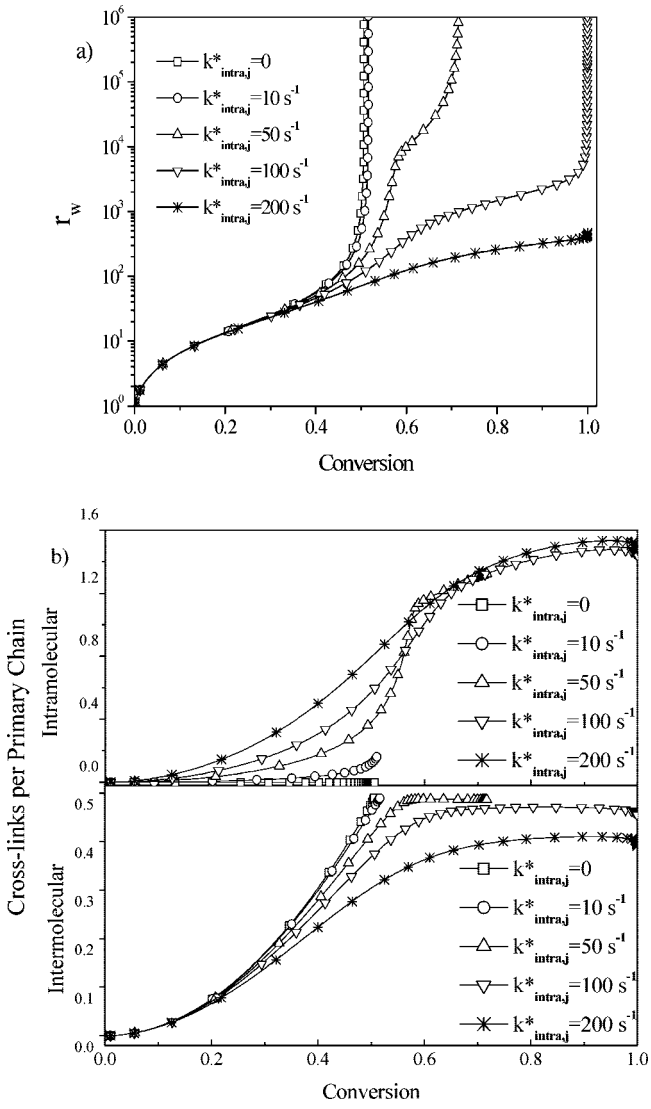

Figure 5. Effect of intramolecular cyclization on gelation: (a) r_w versus monomer conversion and (b) the numbers of intermolecular and intramolecular cross-links per primary chain versus monomer conversion. $[M_1]_0 = 6$ mol/L, $[\text{RAFT}]_0 = 2\%[M_1]_0$, $[M_2]_0 = 4\%[M_1]_0$, and $[I]_0 = 0.2\%[M_1]_0$.

have the smallest value of $k^*_{\text{intra},j}$ because the structure of this cross-linker is bulkier and less flexible than those of the other two. Therefore, by measuring the gel conversion with different copolymerization recipes and comparing the experimental data with this gel diagram, one can effectively estimate the $k^*_{\text{intra},j}$ value.

Recently, Matyjaszewski and coworkers[45] copolymerized MA and EGDA by the ATRP technique and observed that the gel point also depends on the initial concentration of MA. Here we investigate the effect of the solvent on the gel conversion in the RAFT cross-linking process by adjusting the initial vinyl concentration, $[M_1]_0$. Figure 7 shows that $x_{1,\text{gel}}$ is independent of $[M_1]_0$ when there is no intramolecular cyclization. In contrast, when $k^*_{\text{intra}} > 0$, the gel point is postponed when the polymerization system becomes dilute. The $x_{1,\text{gel}}$ value is not very sensitive to the variation in $[M_1]_0$ in the concentrated region (i.e., $[M_1]_0 > 6$ mol/L). However, the gel point is dramatically postponed with the decrease in $[M_1]_0$ in the dilute region (i.e., $[M_1]_0 < 4$ mol/L). From the mechanism, we can see that the intermolecular cross-linking is a bimolecular reaction, whereas the intramolecular cyclization is a monomolecular reaction. The intermolecular cross-linking is therefore more sensitive to the variation in monomer concentration. The ratio of intramolecular

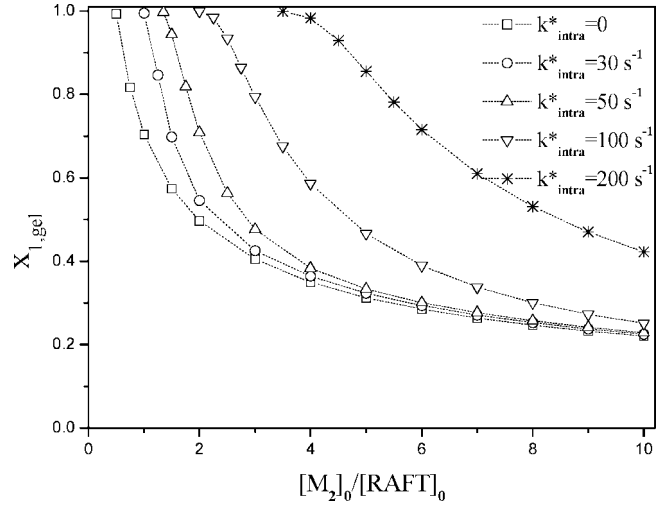

Figure 6. Effect of intramolecular cyclization on the gel conversion at different $[M_2]_0/[\text{RAFT}]_0$ levels. $[M_1]_0 = 6$ mol/L and $[I]_0 = 0.2\%[M_1]_0$.

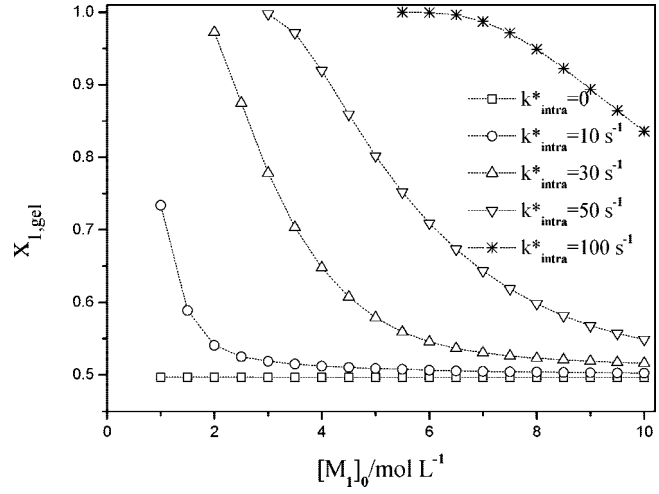

Figure 7. Effect of solvent on the gel conversion. $[\text{RAFT}]_0 = 2\%[M_1]_0$, $[M_2]_0 = 4\%[M_1]_0$, and $[I]_0 = 0.2\%[M_1]_0$.

cyclization and intermolecular cross-linking rates increases when $[M_1]_0$ decreases. As a result, the effect of intramolecular cyclization is more significant when the polymerization system is dilute, which accords with the previous experimental observations.

Branching Development and Distribution. Recently, the synthesis of highly branched macromolecules by controlled/living radical cross-linking has attracted great interest. This kind of macromolecule has a large number of functional groups, which can be further modified for biological applications such as drug delivery. However, it is rather difficult to estimate the average number of branches and the branching distribution by experiment. In this section, we theoretically investigate the branching development and distribution to provide some understanding of the branching process and guidance for the design of hyperbranched materials.

Figure 8a shows the evolution of weight- and number-average branching densities, B_w and B_n, respectively. B_w and B_n equal zero if all of the macromolecules are linear primary chains. In the case of $[M_2]_0/[\text{RAFT}]_0 = 2$, B_w increases very quickly at the vicinity of the gel point and finally diverges. This development of B_w indicates that the highly branched chains are formed close to the gel point if gelation occurs. In contrast, in the absence of gelation, B_w increases significantly at only the end

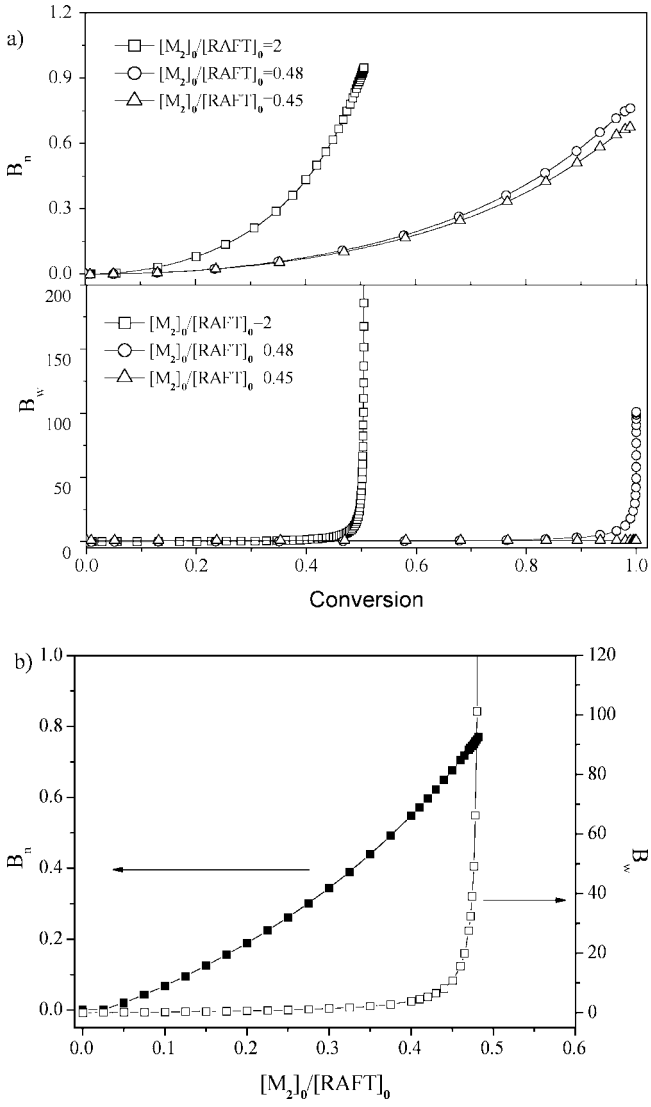

Figure 8. Branching development in the RAFT cross-linking process: (a) number-average branching density (B_n) and weight-average branching density (B_w) versus monomer conversion and (b) B_n and B_w versus $[M_2]_0/[RAFT]_0$ at the complete monomer conversion. $[M_1]_0 = 6$ mol/L, $[RAFT]_0 = 2\%[M_1]_0$, $[I]_0 = 0.2\%[M_1]_0$, and $k^*_{intra,j} = 0$.

of polymerization and finally approaches 102 when $[M_2]_0/[RAFT]_0 = 0.48$ and 11 when $[M_2]_0/[RAFT]_0 = 0.45$. This indicates that the hyperbranched macromolecules are formed in the final stage in the branching/cross-linking process when gelation does not occur. Unlike the abrupt change in B_w, the number-average branching density, B_n, steadily increases with the monomer conversion. In addition, B_n varies in the range of 0 to 1, which indicates that, as far as the number fraction is concerned, the products contain most linear primary and slightly branched chains. The effect of $[M_2]_0/[RAFT]_0$ on B_w and B_n is further illustrated in Figure 8b. It can be clearly seen that B_w is not sensitive to $[M_2]_0/[RAFT]_0$ when its value is small. However, B_w rapidly increases when $[M_2]_0/[RAFT]_0$ approaches its critical value for gelation (i.e., 0.5). Highly branched macromolecules with B_w values larger than 100 can be produced by the use of the recipe of $[M_2]_0/[RAFT]_0 \geq 0.48$. B_n is maintained in the range of 0 to 1 for all of the $[M_2]_0/[RAFT]_0$ values. More importantly, through Figure 8b, one can find the recipe for the product with a targeted degree of branching density.

The above model based on the method of moments can provide only average information on branching. To get the full branching distribution, a more sophisticated model must be

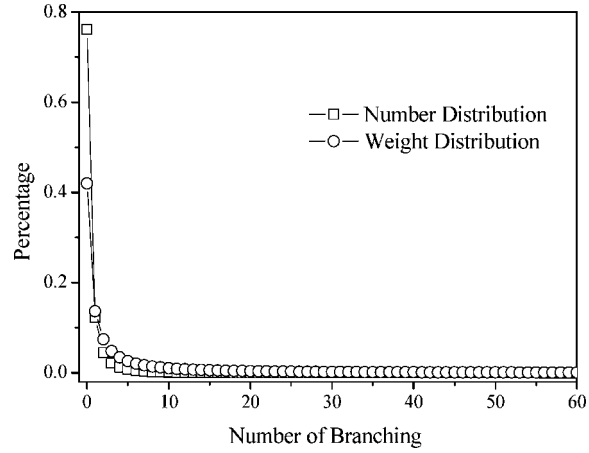

Figure 9. Number and weight distributions of branching in the cross-linking process at 100% monomer conversion. $[RAFT]_0 = 2\%[M_1]_0$, $[M_2]_0/[RAFT]_0 = 0.48$, $[I]_0 = 0.2\%[M_1]_0$, and $k^*_{intra,j} = 0$.

developed. First, we employ the monoradical assumption, the validity of which in the RAFT cross-linking process is proved in the Appendix. To reduce the dimension of variables further, we assume the monodistribution of primary chain length because of the nature of controlled/living radical polymerization. With these simplifications, the population balance can be written as

$$\frac{d[R_N]}{dt} = -k_{tc}[R_N]\sum_{M=1}^{\infty}[R_M] - k_{td}[R_N]\sum_{M=1}^{\infty}[R_M] + k_{tr}(N+1)[D_{N+1}]\sum_{M=1}^{\infty}[R_M] - k_{tr}[R_N]\sum_{M=1}^{\infty}M[D_M] + \sum_{M=1}^{N-1}k^*_M M\bar{r}_{n,0}[D_M][R_{N-M}] - \sum_{M=1}^{\infty}k^*_M M\bar{r}_{n,0}[D_M][R_N] \quad (14a)$$

$$\frac{d[D_N]}{dt} = \frac{1}{2}k_{tc}\sum_{M=1}^{N-1}[R_M][R_{N-M}] + k_{td}[R_N]\sum_{M=1}^{\infty}[R_M] + k_{tr}[R_{N+1}]\sum_{M=1}^{\infty}M[D_M] - k_{tr}N[D_N]\sum_{M=1}^{\infty}[R_M] - k^*_N N\bar{r}_{n,0}[D_N]\sum_{M=1}^{\infty}[R_M] \quad (14b)$$

where R_N denotes the macromolecules with a radical center and D_N stands for the macromolecules with RAFT moieties as their chain ends. The subscript N denotes the number of primary chains involved in the macromolecules. k^*_N is the pseudo rate constant of propagation with pendant double bonds in D_N. In the case in which the reactivity of pendant double bonds is not affected by branching, k^*_N equals k_{inter} and does not depend on N. Using the parameters listed in Table 4, we can solve the above ODEs and obtain the full distribution of R_N and D_N. The number and weight distribution of branching is illustrated in Figure 9. We choose the recipe, $[M_2]_0/[RAFT]_0 = 0.48$ to avoid gelation in the cross-linking process. It can be clearly seen in Figure 9 that both number and weight distributions monotonously decay with the increase in the number of branches. Primary chains consist of 76% in the number fraction and 42% in the weight fraction. The distribution of branched chains is rather broad with a very small fraction of macromolecules having a high number of branches. Highly branched macromolecules are more likely to contain radicals and a larger number of pendant double bonds. The cross-linking reactions between highly branched chains more readily occur. As a result, a large number of primary chains remain in the final product, and the branching distribution becomes broad.

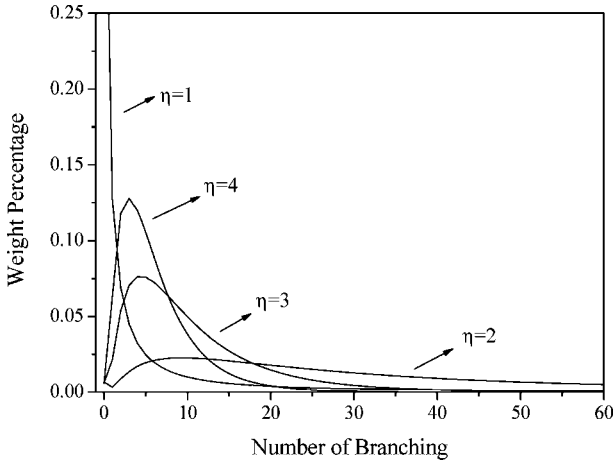

Figure 10. Weight distribution of branching in the RAFT cross-linking process when the reactivity of the pendant double bond is diffusion controlled. $[M_1]_0 = 6$ mol/L, $[\text{RAFT}]_0 = 2\%[M_1]_0$, $[M_2]_0/[\text{RAFT}]_0 = 2$, $[I]_0 = 0.2\%[M_1]_0$, and $k^*_{\text{intra}} = 0$. The percentages are the values at 100% monomer conversion.

However, in the real cross-linking process, pendant double bonds are often trapped inside highly branched macromolecules, which affects their access to radical centers and thus reduced their apparent reactivity. This local heterogeneity is expected to inhibit the further cross-linking of highly branched chains and narrow the branching distribution. Here we consider this local heterogeneity by assuming that k^*_N is diffusion controlled and decreases with the number of branches in a power low form

$$k^*_N = k_{\text{inter}} N^{-\eta} \tag{15}$$

where η determines the dependence of k^*_N on N. The simulation results are shown in Figure 10. It can be clearly seen that primary chains are effectively converted to branched chains when η increases. In addition, the branching distribution becomes narrower when $\eta > 2$. This diffusion-controlled cross-linking mechanism facilitates the control of the branching process. This theoretical suggestion is practically feasible in experiment. Recently, Matyjaszewski et al.[59] have successfully obtained branched macromolecules with very low polydispersity by using an arm-first approach. The long arms that are synthesized before the addition of a cross-linker serve as a shell, which prevents pendant double bonds in the core area from further cross-linking. Their experimental data agree with our theoretical findings that the branching distribution can be fine-tuned by enhancing the local heterogeneity of a cross-linking system.

Conclusions

In this article, we develop a kinetics model on the basis of the method of moments to investigate the RAFT branching/cross-linking process. The following conclusions are reached: (1) The RAFT process has significant effect on gelation. The gel point is postponed by increasing the RAFT agent concentration in the initial recipe. The gel point also depends on the chain transfer coefficient C_{tr}. However, the gel conversion is independent of the radical concentration in the RAFT process. In all cases, Flory's criterion, $\rho r_{\text{w},0} = 1$, is a good approximation for predicting the gel point in the RAFT cross-linking process if the intramolecular cyclization is absent. (2) On the basis of Flory's criterion, the gel conversion in the RAFT cross-linking process can be analytically expressed as

$$[M_2]_0/[\text{RAFT}]_0 = (1/2)[(\alpha-\beta)/(\alpha\beta)][((1-x_{1,\text{gel}})^{\alpha}/\alpha) - ((1-x_{1,\text{gel}})^{\beta}/\beta) + ((\alpha-\beta)/\alpha\beta)]^{-1}$$

The gel conversion decreases monotonously with $[M_2]_0/[\text{RAFT}]_0$. Gelation occurs earlier when the relative reactivities of the divinyl and pendant double bond increase. Using this equation, we can readily estimate the gel point and optimize the cross-linking recipe. (3) The gel point is postponed when intramolecular cyclization is involved. The accumulation of intramolecular cross-links becomes significant after the formation of highly branched macromolecules and greatly suppresses the combination of different chains. The critical value of $[M_2]_0/[\text{RAFT}]_0$ that is required for gelation also increases when the intramolecular cyclization becomes significant. The postponement of gel point becomes more obvious in dilute polymerization systems. (4) Highly branched polymer chains can be formed in only the vicinity of the gel point (in the presence of gelation) or in the final stage of the branching/cross-linking process (in the absence of gelation). The branching distribution is very broad with a large fraction of linear primary and slightly branched chains. However, when the effect of local heterogeneity on the reactivity of the pendant double bond is taken into account, the branching distribution becomes narrower and can be fine-tuned.

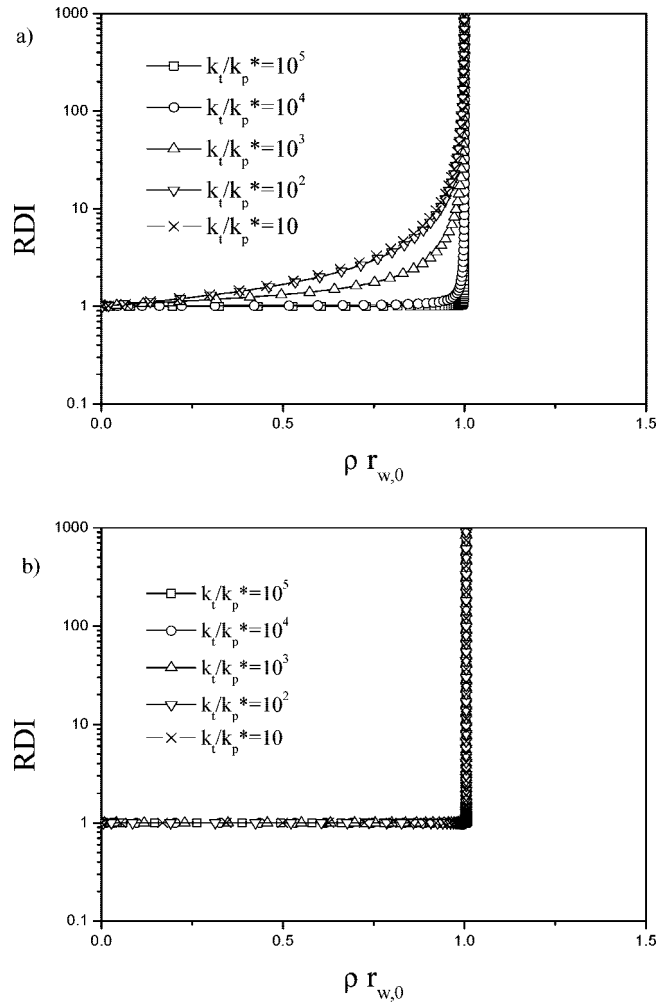

Figure 11. Effect of k_t/k^*_p on the radical distribution index. (a) $[\text{RAFT}]_0 = 0$ and (b) $[\text{RAFT}]_0 = 2\%[M_1]_0$. $[M_1]_0 = 6$ mol/L, $[M_2]_0 = 2\%[M_1]_0$, and $[I]_0 = 0.2\%[M_1]_0$.

Acknowledgment. We would like to thank the NSF of China for a JB Award, the Ministry of Education of China for a Changjiang Scholar Visiting Fellowship as well as for New Century Excellent Talent in University, and Zhejiang University for supporting this research.

Appendix: Radical Distribution in the RAFT Cross-Linking Process

It is well known that the monoradical assumption is often employed in deriving cross-linking models; that is, no macromolecules are allowed to have more than one radical center. Here we investigate the radical distribution in the RAFT cross-linking process and also show the results of the conventional radical cross-linking process for comparison. The formation of polyradical macromolecules is reflected by the radical distribution index (RDI), which is defined as $Y_{0,2,0}/Y_{0,1,0}$. The physical meaning of RDI is the broadness of radical distribution, and it equals unity for a monoradical system. It can be seen that for both conventional (Figure 11a) and RAFT (Figure 11b) cross-linking processes, RDI is close to unity in the early stage, indicating that the macromolecular radicals are mainly monoradicals. Polyradical macromolecules accumulate in a rather sudden manner at the vicinity of the gel point, implying that the gel molecule is likely to have a large number of radical centers. Therefore, it is fair to say that the gel formation in both conventional and RAFT radical cross-linking processes is inherently linked to the existence of polyradical macromolecules. Zhu et al.[21] suggested that in the conventional radical cross-linking process the radical distribution is dependent on a group parameter, k_t/k_p^*. k_t affects the radical concentration, whereas k_p^* determines the cross-linking rate and the number of macromolecules. It is more probable for the presence of polyradical chains when the k_t/k_p^* value is small. We adjust k_t/k_p^* for four orders of magnitude, which covers the possible range of its value in the real polymerization systems, and we find that the dependence of radical distribution on k_t/k_p^* shows a significant difference between the conventional radical and the RAFT cross-linking processes. Figure 11a shows that the evolution of RDI in the conventional radical polymerization is affected by the variation in k_t/k_p^*. RDI remains unity until the vicinity of the gel point if k_t/k_p^* is adequately large, whereas it deviates from unity in a much earlier stage if $k_t/k_p^* < 10^4$. These results are in good agreement with Zhu's previous work. However, in the RAFT system (as shown in Figure 11b), the behavior of radical distribution is not sensitive to the variation in k_t/k_p^*. For all of the k_t/k_p^* values, the RDI diverges only when $\rho r_{w,0} = 1$, indicating that the polyradical macromolecules do not appear until the gel point. As a result, in the RAFT cross-linking process, the monoradical assumption is valid in the pregelation period. The different radical distribution behaviors of the conventional and RAFT processes can be explained by the fact that the concentrations of primary chains as well as macromolecules in the RAFT polymerization are much higher than those in the conventional system. It is thus more likely to form polyradical macromolecules in the conventional radical cross-linking process than in its RAFT counterpart.

References and Notes

(1) Boggs, L. J.; Rivers, M.; Bike, S. G. *J. Coat. Technol.* **1996**, *68*, 63–74.
(2) Flory, P. J. *Principles of Polymer Chemistry*; Cornell University Press: Ithaca, NY, 1953.
(3) Patrickios, C. S.; Georgiou, T. K. *Curr. Opin. Colloid Interface Sci.* **2003**, *8*, 76–85.
(4) Erdodi, G.; Kennedy, J. P. *Prog. Polym. Sci.* **2006**, *31*, 1–18.
(5) Yoshida, R.; Sakai, K.; Okano, T.; Sakurai, Y. *Adv. Drug Delivery Rev.* **1993**, *11*, 85–108.
(6) Langer, R.; Peppas, N. A. *AIChE J.* **2003**, *49*, 2990–3006.
(7) Oh, J. K.; Drumright, R.; Siegwart, D. J.; Matyjaszewski, K. *Prog. Polym. Sci.* **2008**, *33*, 448–477.
(8) (a) Flory, P. J. *J. Am. Chem. Soc.* **1941**, *63*, 3083–3090. (b) Flory, P. J. *J. Am. Chem. Soc.* **1941**, *63*, 3091–3096. (c) Flory, P. J. *J. Am. Chem. Soc.* **1941**, *63*, 3096–3100. (d) Flory, P. J. *J. Am. Chem. Soc.* **1947**, *69*, 2893–2899.
(9) (a) Stockmayer, W. H. *J. Chem. Phys.* **1943**, *11*, 45–55. (b) Stockmayer, W. H. *J. Chem. Phys.* **1944**, *12*, 125–131. (c) Stockmayer, W. H. *J. Chem. Phys.* **1945**, *13*, 199–207.
(10) Charlesby, A.; Pinner, S. H. *Proc. R. Soc. London* **1959**, *A249*, 367–386.
(11) Gordon, M. *Proc. R. Soc. London* **1962**, *A268*, 240–256.
(12) Saito, O. In *The Radiation Chemistry of Macromolecules*; Dole, M., Ed.; Academic Press: New York, 1972.
(13) Macosko, C. W.; Miller, D. R. *Macromolecules* **1976**, *9*, 199–206.
(14) Miller, D. R.; Macosko, C. W. *Macromolecules* **1976**, *9*, 206–211.
(15) Pearson, D. S.; Graessley, W. W. *Macromolecules* **1978**, *11*, 528–533.
(16) Durand, D.; Bruneau, C. M. *Makromol. Chem.* **1982**, *183*, 1007–1020.
(17) Mikos, A. G.; Takoudis, C. G.; Peppas, N. A. *Macromolecules* **1986**, *19*, 2174–2182.
(18) Tobita, H.; Hamielec, A. E. *Makromol. Chem., Macromol. Symp.* **1988**, *20/21*, 501–543.
(19) Tobita, H.; Hamielec, A. E. *Macromolecules* **1989**, *22*, 3098–3105.
(20) Tobita, H.; Hamielec, A. E. *Polymer* **1992**, *33*, 3647–3657.
(21) Zhu, S.; Hamielec, A. E. *Macromolecules* **1993**, *26*, 3131–3136.
(22) Zhu, S. *J. Polym. Sci., Part B: Polym. Phys.* **1996**, *34*, 505–516.
(23) Zhu, S.; Hamielec, A. E. *Macromolecules* **1992**, *25*, 5457–5464.
(24) Walling, C. J. *J. Am. Chem. Soc.* **1945**, *67*, 441–447.
(25) Landin, D. T.; Macosko, C. W. *Macromolecules* **1988**, *21*, 846–851.
(26) Zhu, S.; Tian, Y.; Hamielec, A. E.; Eaton, D. R. *Polymer* **1990**, *31*, 154–159.
(27) Ulbrich, K.; Dusek, K.; Ilavsky, M.; Kopecek, J. *Eur. Polym. J.* **1978**, *14*, 45–49.
(28) Okay, O. *Makromol. Chem.* **1988**, *189*, 2201–2217.
(29) Bastide, J.; Leibler, L. *Macromolecules* **1988**, *21*, 2647–2649.
(30) Kannurpatti, A. R.; Anseth, J. W.; Bowman, C. N. *Polymer* **1998**, *39*, 2507–2513.
(31) Matyjaszewski, K.; Gaynor, S.; Wang, J. S. *Macromolecules* **1995**, *28*, 2093–2095.
(32) Davis, K. A.; Matyjaszewski, K. *Adv. Polym. Sci.* **2002**, *159*, 1–166.
(33) Matyjaszewski, K. *Prog. Polym. Sci.* **2005**, *30*, 858–875.
(34) Braunecker, W. A.; Matyjaszewski, K. *Prog. Polym. Sci.* **2007**, *32*, 93–146.
(35) Goto, A.; Fukuda, T. *Prog. Polym. Sci.* **2004**, *29*, 329–385.
(36) Ide, N.; Fukuda, T. *Macromolecules* **1997**, *30*, 4268–4271.
(37) Ide, N.; Fukuda, T. *Macromolecules* **1999**, *32*, 95–99.
(38) Yu, Q.; Zeng, F.; Zhu, S. *Macromolecules* **2001**, *34*, 1612–1618.
(39) Wang, A. R.; Zhu, S. *Macromolecules* **2002**, *35*, 9926–9933.
(40) Wang, A. R.; Zhu, S. *Polym. Eng. Sci.* **2005**, *45*, 720–727.
(41) Jiang, C. F.; Yu, Q.; Shen, Y. Q.; Zhu, S.; Hunkeler, D. *J. Polym. Sci., Part A: Polym. Chem.* **2001**, *39*, 3780–3788.
(42) Yu, Q.; Zhang, J. Z.; Cheng, M. L.; Zhu, S. *Macromol. Chem. Phys.* **2006**, *207*, 287–294.
(43) Yu, Q.; Zhu, Y. S.; Ding, Y. H.; Zhu, S. *Macromol. Chem. Phys.* **2008**, *209*, 551–556.
(44) Gao, H. F.; Min, K.; Matyjaszewski, K. *Macromolecules* **2007**, *40*, 7763–7770.
(45) Gao, H. F.; Li, W. W.; Matyjaszewski, K. *Macromolecules* **2008**, *41*, 2335–2340.
(46) Li, Y.; Armes, S. P. *Macromolecules* **2005**, *38*, 8155–8162.
(47) Isaure, F.; Cormack, P. A. G.; Graham, S.; Sherrington, D. C.; Armes, S. P.; Buetuen, V. *Chem. Commun.* **2004**, *1138*, 1139.
(48) Bannister, I.; Billingham, N. C.; Armes, S. P.; Rannard, S. P.; Findlay, P. *Macromolecules* **2006**, *39*, 7483–7492.
(49) Vo, C. D.; Rosselgong, J.; Armes, S. P.; Billingham, N. C. *Macromolecules* **2007**, *40*, 7119–7125.
(50) Liu, B.; Kazlauciunas, A.; Guthrie, J. T.; Perrier, S. *Macromolecules* **2005**, *38*, 2131–2136.
(51) Achilleos, M.; Christoforou, T. K.; Patrickios, C. S. *Macromolecules* **2007**, *40*, 5575–5581.
(52) Barner-Kowollik, C.; Quinn, J. F.; Morsley, D. R.; Davis, T. P. *J. Polym. Sci., Part A: Polym. Chem.* **2001**, *39*, 1353–1365.
(53) Kwak, Y.; Goto, A.; Fukuda, T. *Macromolecules* **2004**, *37*, 1219–1225.
(54) Luo, Y. W.; Wang, R.; Yang, L.; Yu, B.; Li, B. G. ; Zhu, S. *Macromolecules* **2006**, *39*, 1328–1337.
(55) Odian, G. *Principles of Polymerization*, 4th ed.; Wiley-Interscience: Hoboken, NJ, 2004.
(56) Beuermann, S.; Buback, M. *Prog. Polym. Sci.* **2002**, *27*, 191–254.
(57) Chong, Y. K.; Krstina, J.; Le, T. P. T.; Moad, G.; Postma, A.; Rizzardo, E.; Thang, S. H. *Macromolecules* **2003**, *36*, 2256–2272.
(58) Monteiro, M. J.; de Brouwer, H. *Macromolecules* **2001**, *34*, 349–352.
(59) Gao, H. F.; Matyjaszewski, K. *Macromolecules* **2008**, *41*, 4250–4257.

MA802006C